

Formation, detection, and stability studies of neutral vanadium sulfide clusters

Sheng-Gui He, Yan Xie, Yuanqing Guo, and Elliot R. Bernstein

Citation: [The Journal of Chemical Physics](#) **126**, 194315 (2007); doi: 10.1063/1.2730828

View online: <http://dx.doi.org/10.1063/1.2730828>

View Table of Contents: <http://aip.scitation.org/toc/jcp/126/19>

Published by the [American Institute of Physics](#)

COMPLETELY
REDESIGNED!



PHYSICS
TODAY

Physics Today Buyer's Guide
Search with a purpose.

Formation, detection, and stability studies of neutral vanadium sulfide clusters

Sheng-Gui He, Yan Xie, Yuanqing Guo, and Elliot R. Bernstein

Department of Chemistry, Colorado State University, 1872 Campus Delivery, Fort Collins, Colorado 80523

(Received 25 January 2007; accepted 23 March 2007; published online 21 May 2007)

Neutral vanadium sulfide clusters are generated by the reaction of seeded hydrogen sulfide in a helium carrier gas with laser ablated vanadium metal within a supersonic nozzle. The exiting clusters are expanded into a vacuum in a molecular beam and are ionized by both ultraviolet (UV) and vacuum UV (VUV) laser radiation. The generated ions are detected by a time of flight mass spectrometer. With single photon ionization (SPI) employing VUV (118 nm) radiation, sulfur rich clusters (V_mS_n , $n > m+1$) and hydrogen containing clusters ($V_mS_nH_x$, $x > 0$) are observed. With multiphoton ionization (MPI) through nanosecond UV (193 nm) radiation, these sulfur rich and hydrogen containing clusters cannot be observed, indicating severe fragmentation generated by MPI and the importance of SPI in determining the neutral vanadium sulfide cluster distribution. With MPI through femtosecond UV (226 nm) radiation, a few sulfur rich and hydrogen containing clusters are detected, but most clusters observed by SPI are still undetected even by femtosecond MPI. Density functional theory calculations are applied to optimize energies and structures of the clusters with $m=1-3$ and $n=0-7$. The experimental results are well interpreted based on the calculations. The calculated and experimental results for vanadium sulfides are compared with those of vanadium oxides in literature. © 2007 American Institute of Physics. [DOI: [10.1063/1.2730828](https://doi.org/10.1063/1.2730828)]

I. INTRODUCTION

Gas phase transition metal containing clusters (such as carbides, nitrides, oxides, sulfides, etc.) are excellent model systems upon which to base a fundamental understanding of condensed phase and surface properties, chemistry, and dynamics. On the other hand, these clusters offer a challenge for theoretical modeling and computation of their energetics, structures, and electronic states.^{1,2} Among these clusters, charged species^{3,4} have been much more extensively studied than neutral ones because electric and magnetic forces can be used to control and manipulate charged particles; in contrast, neutral clusters are difficult to control and usually must be ionized for detection.

Cluster electronic and reactivity properties should depend sensitively on charge state, especially for small clusters. Neutral cluster properties are important to study in order to have a complete understanding of a cluster, and by implication, of condensed phase and surface chemistry. We have studied neutral cluster distributions and reactivity employing single photon ionization (SPI) with vacuum ultraviolet (VUV) and soft x-ray lasers.⁵⁻¹⁰ SPI is essential for detecting neutral oxide cluster distributions through time of flight mass spectrometry (TOFMS), while multiphoton ionization (MPI) through 193 and/or 355 nm laser radiation can never detect a complete oxide cluster distribution due to (sometimes severe) photodissociation during or after ionization. SPI has also been used by us to study successfully the reactivity of a few groups of metal oxide clusters.¹¹ With this present work, studies have been extended to metal sulfide clusters. In this paper, we explore the formation, detection, and stability of neutral vanadium sulfide clusters. This work is also

motivated by the fact that bulk vanadium sulfide is a good catalyst for hydrogenation reactions of various cyclic molecules.^{12,13} The study of gas phase vanadium sulfide clusters can thus finally shed light on the molecular level mechanisms for bulk catalytic reactions.

Previous experimental work on gas phase vanadium sulfide clusters is mostly for monovanadium polysulfide cations (VS_n^+ , $n=1-10$).¹⁴⁻¹⁸ Cationic¹⁹ and anionic^{19,20} clusters with up to 14 vanadium atoms have been produced by laser ablation of vanadium/sulfur powder mixtures or V_2S_3 samples. A 248 nm photodissociation¹⁹ has also been used to study the stability of $V_mS_n^+$ clusters. Sulfur rich clusters ($n > m$) are suggested to be composed of a kernel $V_mS_n^+$ and $n-m$ peripheral sulfur atoms that are easy to lose as S_2 , S_4 (or S_2+S_2), or S_6 (or $S_2+S_2+S_2$) units upon UV photon absorption. In addition, $V_2S_2^+$, $V_3S_4^+$, and $V_4S_4^+$ are found to have relatively high stability. Spectroscopy of VS in the gas phase and VS_2 in an argon matrix can be found in Refs. 21 and 22, respectively. Quantum chemistry calculations of structures and vibrational frequencies are also reported for VS_n^+ ,^{15,17,18,23,24} $V_2S_2^+$ and $V_3S_4^+$,²⁵ and VS and VS_2 .²²

In the present work, neutral V_mS_n clusters are produced and detected by MPI and SPI techniques. Density functional theory (DFT) calculations are applied to small clusters ($m < 4$ and $n < 8$). The following questions are addressed in these studies: (1) is SPI, employing a VUV laser, able to and necessary to study neutral V_mS_n cluster distribution and reactivity; (2) how are the vanadium and sulfur atoms bonded to form a cluster; and (3) how different are sulfide (V_mS_n) and oxide (V_mO_n) cluster molecules of vanadium?

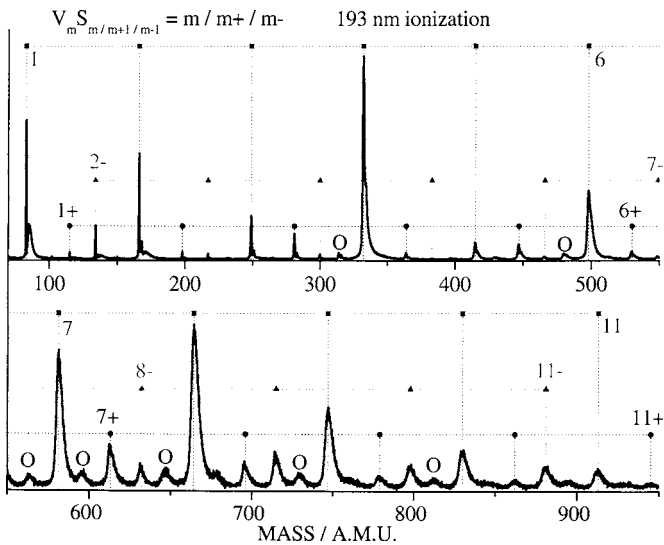


FIG. 1. TOF mass spectrum of vanadium sulfide clusters generated by multiphoton ionization through 193 nm radiation. 5% H₂S seeded in 5 atm He is used as the expansion gas. Three series of clusters V_mS_m , V_mS_{m+1} , and V_mS_{m-1} are observed and are marked by solid square, circle, and up triangle symbols, respectively. The peaks marked with O are due to oxygen impurities.

II. EXPERIMENTAL PROCEDURES

The pulsed laser ablation/supersonic nozzle apparatus employed in this work has been discussed in Ref. 26 and a few more details can be found in Ref. 27. Only a brief outline of the experiments is given below. V_mS_n clusters are generated by laser ablation of a vanadium metal foil in the presence of a helium carrier gas seeded with various concentrations of H₂S. CS₂ is also used instead of H₂S in the carrier gas in order to test the synthesis of V_mS_n species in the experiment. The clusters formed in a gas channel (Φ2 mm × 33 mm) are expanded and skimmed (Φ2 mm) into a vacuum system of a TOFMS for ionization through three different lasers: a 193 nm UV excimer (ArF) laser with a pulse width of ~10 ns, a 226 nm UV femtosecond laser with a pulse width of ~200 fs, and a 118 nm VUV laser with a pulse width of ~5 ns. Ions are detected and signals are recorded as previously described.²⁶ The 118 nm laser light is generated by focusing the third harmonic (355 nm, ~30 mJ) of a Nd:YAG (yttrium aluminum garnet) laser in a tripling cell that contains about a 250 Torr argon/xenon (10/1) gas mixture.^{5–9}

III. DFT CALCULATIONS

Becke's exchange²⁸ and Perdew-Wang's correlation²⁹ (BPW91) functionals with a contracted Gaussian basis set of triple zeta valence quality³⁰ plus one *d* function for sulfur and one *p* function for vanadium are used to optimize the structures of V_mS_n with different isomers and spin multiplicities. This basis set is denoted as TZVP in the GAUSSIAN03 program,³¹ which is used in this work for all the calculations. A vibrational frequency calculation is also carried out after each optimization to check that all the frequencies are positive. For each cluster, different initial structures (models) are used as input in the optimization procedure. For each model,

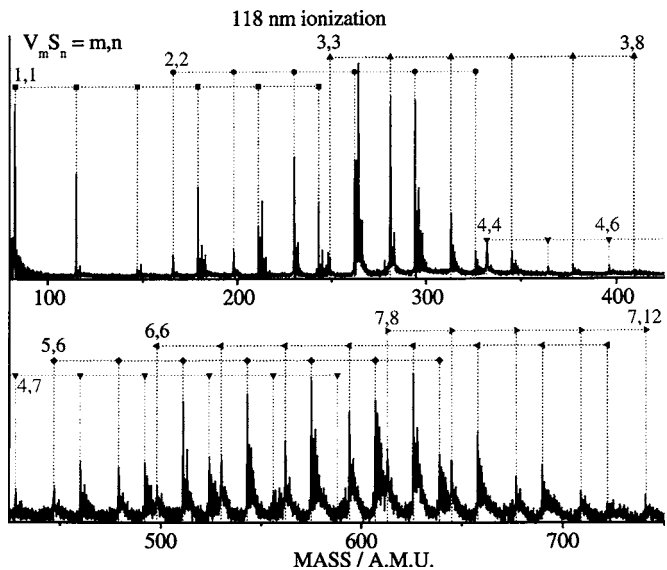


FIG. 2. TOF mass spectrum of vanadium sulfide clusters generated by single photon ionization through 118 nm radiation. 3% H₂S seeded in 5 atm He is used as the expansion gas. The sulfur series are marked by solid square (VS_n), circle (V₂S_n), up triangle (V₃S_n), down triangle (V₄S_n), diamond (V₅S_n), left triangle (V₆S_n), and right triangle (V₇S_n) symbols. The peaks on the high mass side of V_mS_n features correspond to hydrogen containing clusters (V_mS_nH_x, see Fig. 3).

spin multiplicities are scanned from low to high until an energy minimum is found. For sulfur poor clusters (V_mS_n, $n \leq m$), additional one or more high spin multiplicities are also tested because these clusters may have a low energy high spin state. Adiabatic ionization energies (IEs) are also calculated for the lowest energy structure of each cluster. Two spin multiplicities with $M(\text{ion}) = M(\text{neutral}) \pm 1$ are tested in the IE calculation, in which $M(\text{ion})$ and $M(\text{neutral})$ are spin multiplicities of the cation and the neutral species, respectively.

IV. RESULTS

A. Mass spectra of neutral vanadium sulfide clusters

Figure 1 plots the TOF mass spectrum of V_mS_n generated using 5% H₂S in the carrier gas and ionized through the 193 nm (6.4 eV) radiation. Three series of clusters are observed for this experimental condition: an intense V_mS_m and two relatively weak V_mS_{m-1} and V_mS_{m+1}. Various other H₂S concentrations are also used in the 193 nm ionization experiment. The spectra are similar to the one shown in Fig. 1 for H₂S concentrations in the range of 1%–10%. At very low H₂S concentration ($\leq 0.3\%$), sulfur poor clusters V_mS_{m-1} become relatively intense and new series, such as V_mS_{m-2}, are observed. Figure 2 plots the mass spectrum of clusters generated using 3% H₂S and ionized through 118 nm (10.5 eV) radiation. Under these conditions many sulfur rich clusters (V_mS_{m+k}, $k=2–7$), never present in the 193 nm spectrum, are observed. Because H₂S is used as sulfur source in the experiment, many hydrogen containing clusters (V_mS_nH_x, $x \neq 0$) are also observed through 118 nm ionization. Two portions of the spectrum in Fig. 2 are expanded and plotted in Fig. 3. Hydrogen containing clusters are not observable through 193 nm ionization (see Fig. 1). The 118 nm ionized mass

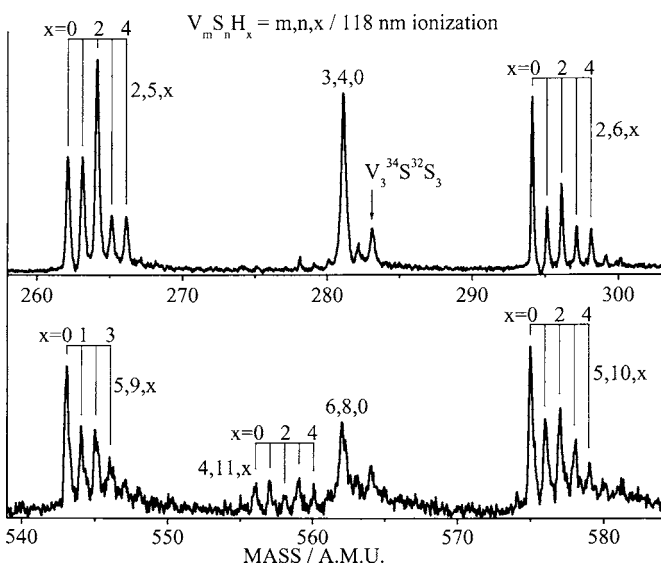


FIG. 3. Selected portions of the TOF spectrum in Fig. 2 showing the hydrogen containing clusters.

spectra under different concentrations of H_2S are shown in Fig. 4. Sulfur rich clusters become less abundant, while sulfur poor clusters become relatively more abundant, as H_2S concentration is decreased. Higher concentrations (up to 10%) of H_2S in the carrier gas are also employed in this work, and the mass spectra for such samples are quite similar to the one shown in Fig. 2, except that the sulfur series (such as V_2S_n and V_3S_n) is longer by one or more sulfur atoms. Figure 5 compares a portion of the mass spectra obtained with different ionization lasers. The result of 226 nm (5.5 eV) femtosecond laser ionization is roughly the same as the result of 193 nm nanosecond laser ionization except a few more sulfur rich (VS_3 , VS_4 , V_2S_4 , and V_3S_5) and hydro-

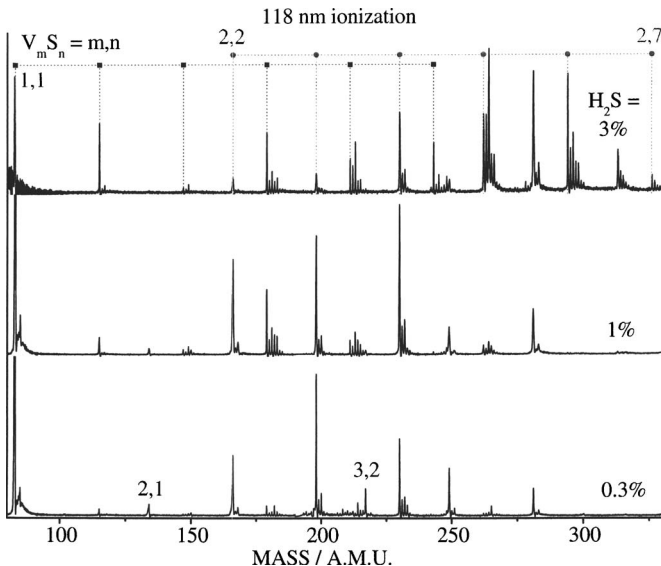


FIG. 4. TOF mass spectra of vanadium sulfide clusters generated by single photon ionization through 118 nm radiation. 3% (top panel), 1% (middle panel), and 0.3% (bottom panel) H_2S seeded in 5 atm He are used as the expansion gas. Two sulfur series of clusters VS_n and V_2S_n are marked by solid square and circle symbols, respectively. The peaks on the high mass side of V_mS_n correspond to hydrogen containing clusters ($\text{V}_m\text{S}_n\text{H}_x$, see Fig. 3).

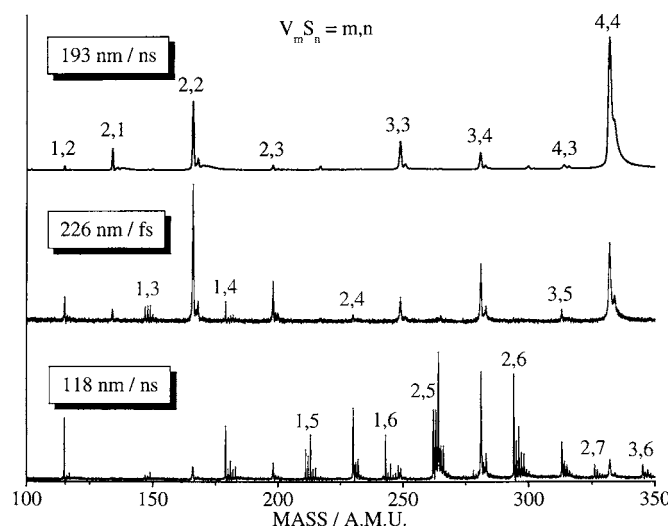


FIG. 5. TOF mass spectra of vanadium sulfide clusters generated by different ionization methods. The spectra in top and bottom panels are portions of the spectra in Figs. 1 and 2, respectively. The spectrum in the middle panel is obtained by ionization through a 226 nm femtosecond laser. The peaks on the high mass side of V_mS_n correspond to hydrogen containing clusters ($\text{V}_m\text{S}_n\text{H}_x$).

gen containing (VS_3H_x , $x=1, 2$, and VS_4H_x , $x=1, 2, 3$) clusters are observed. Figure 6 plots the cluster distribution under 118 nm ionization and using 3% CS_2 as the sulfur precursor seeded in the carrier gas. Pure vanadium sulfide clusters and carbon containing clusters are generated and observed under these experimental conditions. The sulfur series (V_xS_n , x constant and n variable) is not as long as the one generated using 3% H_2S as the sulfur precursor, so CS_2 for a reactant is not a good choice to generate sulfur rich clusters.

B. DFT calculations for vanadium sulfide clusters

To gauge the validity of the BPW91/TZVP method for the calculation of the properties of vanadium sulfide clusters,

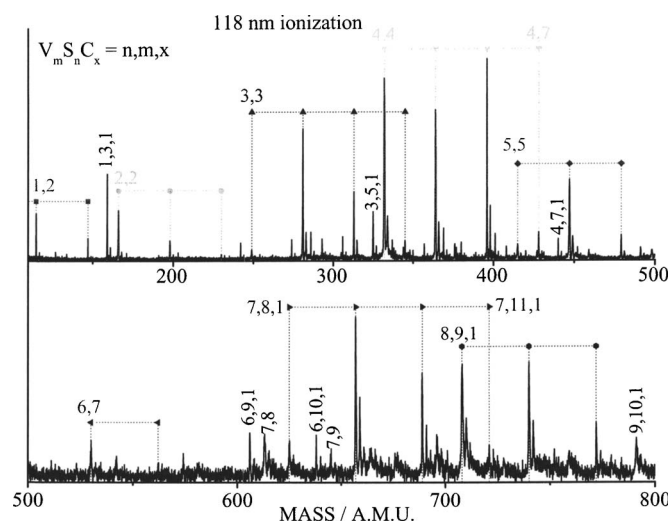


FIG. 6. TOF mass spectrum of vanadium sulfide clusters generated by single photon ionization through 118 nm radiation. 3% CS_2 seeded in 5 atm He is used as the expansion gas. The sulfur containing series are marked by solid square (VS_n), circle (V_2S_n), up triangle (V_3S_n), down triangle (V_4S_n), diamond (V_5S_n), left triangle (V_6S_n), right triangle ($\text{V}_7\text{S}_n\text{C}$), and hexagon ($\text{V}_8\text{S}_n\text{C}$) symbols. The peak on the high mass side of $\text{V}_m\text{S}_n\text{C}_x$ by 2 amu corresponds to $\text{V}_m^{32}\text{S}_{n-1}^{34}\text{SC}_x$.

TABLE I. A comparison of V_2 , VS, S_2 , and S_3 calculated and experimental molecular structures (R in 10^{-10} m and A in deg), vibrational frequency (ω in cm^{-1}), ionization energy (IE in eV), and binding energy (ΔE in eV).

| | Calc. | | | | Expt. ^a | | | |
|-------|--------|----------|------|--------------|--------------------|----------|---------------------|---------------------|
| | R/A | ω | IE | ΔE^b | R/A | ω | IE | ΔE |
| V_2 | 1.7626 | 654.3 | 6.07 | 2.98 | 1.77 | 537.1 | 6.3566 ± 0.0006 | 2.753 ± 0.001 |
| VS | 2.0631 | 538.2 | 7.88 | 4.93 | 2.0501 | 542.14 | 8.4 ± 0.3 | 4.95 ± 0.02 |
| S_2 | 1.9395 | 675.1 | 9.51 | 4.48 | 1.8892 | 725.65 | 9.356 ± 0.002 | 4.3693 ± 0.0009 |
| S_3 | 1.9683 | 624.0 | 9.46 | 6.81 | 1.914 | 676 | 9.68 ± 0.03 | 7.11 ± 0.09 |
| | 118.35 | 557.3 | | | 117.33 | 581 | | |
| | | 248.3 | | | | 281 | | |

^aReferences 21 and 32–39.

^bTo compare with experimental data, zero-point energy corrections are made for V_2 , S_2 , and S_3 and thermal correction to the enthalpy for VS is made.

molecular structure, vibrational frequency, ionization energy, and binding energy calculations are performed for V_2 , VS, S_2 , and S_3 and the results are compared with experimental values,^{21,32–39} as listed in Table I. The experimental bond lengths of V_2 and VS are very well reproduced by the calculation. The calculated bond lengths of S_2 and S_3 are longer than the experimental values by 0.05 Å, probably due to the tight d effect⁴⁰ that is not taken into account by the TZVP basis set used in this work for sulfur. As a result, the calculated vibrational frequencies of S_2 and S_3 are all lower than the experimental values by about 30–50 cm^{-1} . All the calculated ionization energies agree with experimental values within about 0.3 eV. The binding energies also agree with each other within 0.3 eV (~7 kcal/mol). The results indicate that the BPW91/TZVP method is capable of calculating a reasonably good structure for V_mS_n ($m \neq 0$). The calculated relative energies of V_mS_n and $V_mS_n^+$ are believed to be accurate enough to guide a qualitative description of the energetics. In this work, the basis set superposition error⁴¹ (BSSE) due to the use of incomplete basis sets for vanadium and sulfur atoms is not considered in reporting the cluster binding, bond, and dissociation energies. A test calculation indicates that BSSE is about 0.05 eV for VS bond energy, which is negligible compared to the total energy (~5 eV), for our qualitative purposes in this report.

Figures 7 and 8 present the lowest energy structures found for VS_n (top panel of Fig. 7), V_2S_n (bottom panel of Fig. 7), and V_3S_n (Fig. 8). As examples, Fig. 9 shows the results with different structures and spin multiplicities for VS_5 and V_2S_5 . Four different types of vanadium-sulfur bonding are evident from Figs. 7 and 8: (1) terminal V–S bond with a length in the range of 2.03–2.10 Å (V=S character), (2) bridged V–S–V bonding with a V–S bond length in the range of 2.20–2.29 Å, (3) V(S_2) bonding with a V– S_2 distance in the range of 2.24–2.29 Å as found in VS_4 , VS_5 , and VS_6 (sulfur-sulfur bonding is significant in this case), and (4) S≡(3 V) bonding with characteristics of triple bonding between one sulfur and three vanadium atoms (the V–S distance is in the range of 2.30–2.41 Å in this case). Vanadium-vanadium metallic bonding is present in V_2S_n and V_3S_n with $n \leq 5$. The top panel of Fig. 9 shows that for VS_5 the structure with a sulfur-vanadium ring (ring– S_n –V–) is not as stable as the structure with only V–S and V–(S_2)

bondings. This point is also confirmed for VS_4 and VS_6 . Based on this result, no structure with ring– S_n –V– ($n \geq 3$) has been tested in the structure optimization for V_2S_n and V_3S_n . The bottom panel of Fig. 9 shows that an open structure ($C_1/M=1$) is unstable compared to compact structures with more bridged V–S–V bonds. The structure of a V_mS_n cluster is also strongly dependent on the spin state (see Fig. 9, M =multiplicity): (1) VS_5 has a C_s symmetry structure for $M=2$, but the symmetry changes to C_{2v} for $M=4$; (2) V_2S_5 has a D_{3h} structure for $M=1$, but the D_{3h} structure is not stable for $M=3$ and 5, for which the most stable structures have C_s symmetry (if the V_2S_5 optimized structure $C_s/M=3$ is used as the initial input for the structure optimization of V_2S_5 $M=1$, the D_{3h} structure is finally generated); and (3) the terminal V–S bond length increases as M increases, which implies that the unpaired electrons are (at least partially) located in the terminal V–S bonds for a cluster with a high spin multiplicity ($M \geq 3$).

Table II lists the adiabatic ionization energies of V_mS_n clusters. The lower spin state of cationic clusters ($V_mS_n^+$) is usually more stable than the higher one. The exceptions are

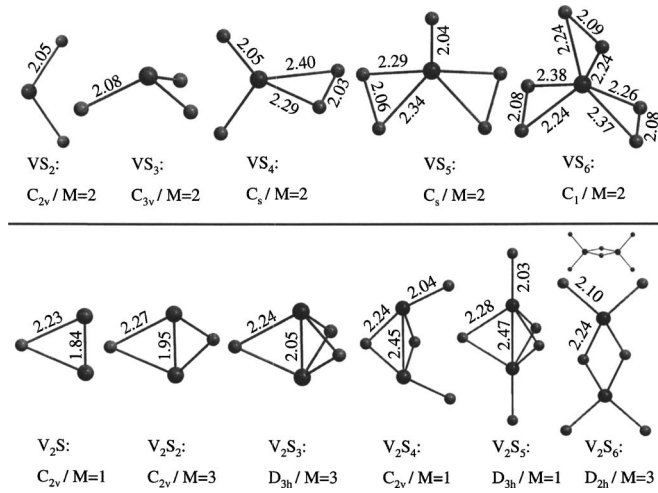


FIG. 7. DFT optimized structures of VS_n (top panel) and V_2S_n (bottom panel). For each cluster, only the lowest energy structure with a symmetry and spin multiplicity (M) is listed. For V_2S_6 , a second angle view is provided to have a better understanding of the geometry. In this figure and Figs. 8 and 9, bigger (gray) and smaller (yellow) balls represent vanadium and sulfur atoms, respectively; the bond length values in Å are given.

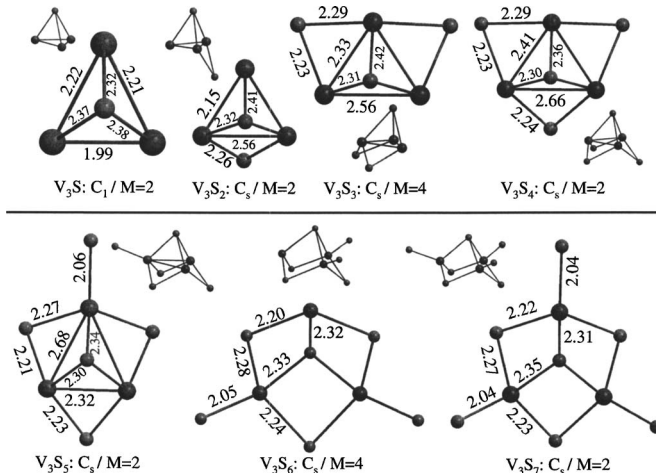


FIG. 8. DFT optimized structures of V_3S_n . For each cluster, only the lowest energy structure with a symmetry and spin multiplicity (M) is listed. A second angle view is also provided to have a better understanding of the geometry.

V_2^+ , $V_2S_6^+$, and $V_3S_6^+$. The IE of V_2S_n and V_3S_n generally increases with the increasing n , which agrees with the structures in Figs. 7 (bottom panel) and 8, in which less V–V metallic bonding is present for clusters with more sulfur atoms. The IE of VS_n increases to a maximum at $n=3$ then decreases as n increases. This suggests that the $V(S_2)$ bonding, as found in VS_4 , VS_5 , and VS_6 (top panel of Fig. 7), tends to generate at least one loosely bound electron in the cluster.

To discuss the stability of V_mS_n clusters, Table III lists the dissociation channels ($V_{i+j}S_{k+l} \rightarrow V_iS_k + V_jS_l$) and energies [$\Delta E = E(V_iS_k) + E(V_jS_l) - E(V_{i+j}S_{k+l})$] for the most stable structures in Figs. 7 and 8. Table IV lists similar results for cationic clusters by using the optimized energies of both $V_mS_n^+$ and V_mS_n . Figure 10 summarizes the lowest dissociation and ionization energies for each cluster using the data from Tables II–IV. From Tables III and IV one concludes that sulfur rich clusters ($V_mS_n^{0/+}$, $n > \sim m$) have the most energetically favorable dissociation channels involving loss of a S_2 or S unit. The dissociation energy has a tendency to decrease as n increases for these sulfur rich clusters. For sulfur poor clusters ($V_mS_n^{0/+}$, $n \leq \sim m$), the most favorable dissociation channels usually involve the loss of a VS or V unit. The lowest dissociation energies have a maximum at $m=n$ ($V_2S_2^+$) or $n=m+1$ (V_2S_3 and $V_3S_4^{0/+}$) for each sulfur

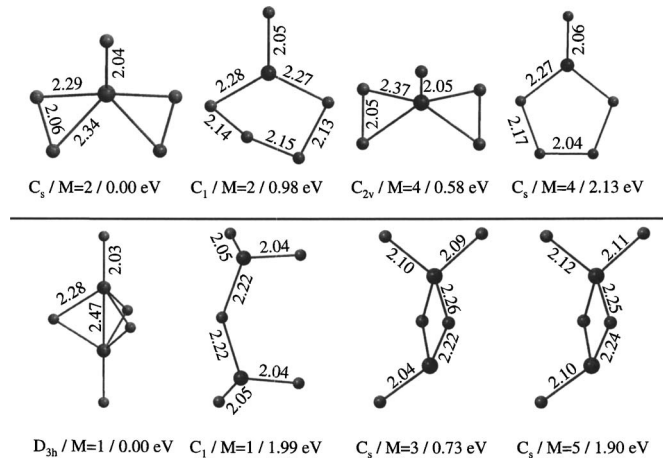


FIG. 9. DFT optimized structures and relative energies of VS_5 (top panel) and V_2S_5 (bottom panel) with different structural models and spin multiplicities (M).

series (Fig. 10, see Tables III and IV for details). Vanadium sulfide clusters V_mS_n with a stoichiometry of $m:n \approx 2:5$ do not possess the highest dissociation energy in each sulfur series (m constant and n variable).

V. DISCUSSION

A. Cluster fragmentation during ionization

Figure 2 shows that sulfur rich clusters (V_mS_n , $n > m+1$) are generated under our experimental conditions, however, none of them can be observed by ionization through 193 nm (6.42 eV) nanosecond laser radiation. Table II indicates that these clusters all have IEs higher than 6.5 eV which requires a MPI process to ionize them. A sufficient photon density must be provided for MPI to occur, and clusters may fragment severely in a high photon fluence. The low dissociation energies of $V_mS_n^{0/+}$ ($n > m+1$) listed in Tables III and IV indicate that cluster fragmentation can occur in both neutral and ion states. The Rice-Ramsberger-Kassel (RRK) model can be used to estimate the rates of fragmentation after the cluster absorbs one photon, employing the following form:

$$k_{\text{dis}} = \nu [1 - \Delta E / (h\nu_{193} + E_v)]^{3N-7}, \quad (1)$$

TABLE II. Calculated adiabatic ionization energy (IE in eV) of V_mS_n (m, n) clusters.

| m, n | IE(L) ^a | IE(H) ^b | m, n | IE(L) ^a | IE(H) ^b | m, n | IE(L) ^a | IE(H) ^b |
|--------|------------------------|------------------------|--------|------------------------|------------------------|--------|------------------------|------------------------|
| 1, 1 | 7.88 | 9.02 | 2, 0 | 6.42 | 6.07 | 3, 0 | 5.33 | 5.61 |
| 1, 2 | 8.33 | 8.70 | 2, 1 | | 6.63 | 3, 1 | 5.75 | 5.62 |
| 1, 3 | 9.09 | 9.18 | 2, 2 | 6.77 | 6.95 | 3, 2 | 5.55 | 6.02 |
| 1, 4 | 8.76 | 9.44 | 2, 3 | 7.31 | 7.89 | 3, 3 | 6.13 | 6.46 |
| 1, 5 | 8.09 | 8.09 | 2, 4 | | 7.93 | 3, 4 | 6.26 | 6.71 |
| 1, 6 | 7.66 | 7.69 | 2, 5 | | 8.61 | 3, 5 | 7.27 | 7.33 |
| | | | 2, 6 | 8.52 | 8.45 | 3, 6 | 7.42 | 8.46 |
| | | | | | | 3, 7 | 7.77 | 8.76 |

^aIE(L) is for $M(\text{ion})=M(\text{neutral})-1$, see text for details.

^bIE(H) is for $M(\text{ion})=M(\text{neutral})+1$, see text for details.

TABLE III. Dissociation channels (only two channels with the lowest dissociation energies are listed for each cluster) and energies (ΔE in eV) of neutral vanadium sulfide clusters.

| | Channel | ΔE | | Channel | ΔE | | Channel | ΔE |
|-----------------|--------------------------|------------|-------------------------------|----------------------------|------------|-------------------------------|-----------------------------|------------|
| VS | $\rightarrow V + S$ | 4.96 | V ₂ S | $\rightarrow VS + V$ | 3.46 | V ₃ S | $\rightarrow V_2S + V$ | 2.91 |
| | | | | $\rightarrow V_2 + S$ | 5.40 | | $\rightarrow V_2 + VS$ | 3.35 |
| VS ₂ | $\rightarrow VS_2 + S$ | 4.45 | V ₂ S ₂ | $\rightarrow 2VS$ | 3.60 | V ₃ S ₂ | $\rightarrow V_2S_2 + V$ | 3.52 |
| | $\rightarrow V + S_2$ | 4.89 | | $\rightarrow VS_2 + V$ | 4.11 | | $\rightarrow V_2S + VS$ | 3.66 |
| VS ₃ | $\rightarrow VS_3 + S_2$ | 3.70 | V ₂ S ₃ | $\rightarrow VS_2 + VS$ | 4.27 | V ₃ S ₃ | $\rightarrow V_2S_3 + V$ | 3.79 |
| | $\rightarrow VS_2 + S$ | 3.77 | | $\rightarrow V_2S_2 + S$ | 5.12 | | $\rightarrow V_2S_2 + VS$ | 3.94 |
| VS ₄ | $\rightarrow VS_2 + S_2$ | 2.70 | V ₂ S ₄ | $\rightarrow 2VS_2$ | 3.95 | V ₃ S ₄ | $\rightarrow V_2S_3 + VS$ | 4.82 |
| | $\rightarrow VS_3 + S$ | 3.45 | | $\rightarrow V_2S_3 + S$ | 4.13 | | $\rightarrow V_2S_2 + VS_2$ | 5.49 |
| VS ₅ | $\rightarrow VS_3 + S_2$ | 2.45 | V ₂ S ₅ | $\rightarrow V_2S_3 + S_2$ | 3.63 | V ₃ S ₅ | $\rightarrow V_3S_4 + S$ | 4.33 |
| | $\rightarrow VS_4 + S$ | 3.51 | | $\rightarrow V_2S_4 + S$ | 4.02 | | $\rightarrow V_2S_3 + VS_2$ | 4.69 |
| VS ₆ | $\rightarrow VS_4 + S_2$ | 1.79 | V ₂ S ₆ | $\rightarrow V_2S_4 + S_2$ | 1.98 | V ₃ S ₆ | $\rightarrow V_3S_4 + S_2$ | 3.71 |
| | $\rightarrow VS_5 + S$ | 2.80 | | $\rightarrow V_2S_5 + S$ | 2.48 | | $\rightarrow V_3S_5 + S$ | 3.91 |
| | | | | | | V ₃ S ₇ | $\rightarrow V_3S_5 + S_2$ | 3.49 |
| | | | | | | | $\rightarrow V_3S_6 + S$ | 4.10 |

$$E_v = (3N - 6)kT_v, \quad (2)$$

in which ΔE is cluster dissociation barrier, simplified as the dissociation energy in Tables III and IV, $h\nu_{193}$ is the photon energy (6.42 eV), N is the number of atoms in the cluster, k is the Boltzmann constant, T_v is the initial cluster vibrational temperature, and ν is the effective frequency along the dissociation coordinate. We assume that the electronic energy given to the cluster by absorption of a photon will convert to cluster vibrational energy prior to cluster dissociation; that is, internal energy conversion and introcluster vibrational energy redistribution (IVR) are much faster than vibrational predissociation. To estimate the dissociation rate (k_{dis}), $T_v = 700$ K is used as determined for VO₂ in Ref. 7 and $\nu = 3 \times 10^{12} \text{ s}^{-1}$ (100 cm⁻¹) is assumed. The calculated dissociation rates are listed in Table V.

The results in Table V indicate that the 193 nm nanosecond (~ 10 ns) laser may never be able to ionize VS_n ($n \geq 3$) because the cluster dissociates within less than 0.1 ns after absorbing the first photon, and thus it has only a small chance to absorb a second photon to get ionized. The situation is similar for V₂S_n ($n \geq 4$), for which the dissociation of

neutral V₂S₄ and V₂S₅ will compete with the ionization (absorbing of the second photon); however, for a sufficient photon density for second photon absorption, the ionized species V₂S₄⁺ and V₂S₅⁺ can further absorb one photon and fragment within less than 0.1 ns. Moreover, the excess energy (part of $xh\nu_{193}\text{-IE}$, $x \geq 2$) left in the ion may cause its fragmentation directly. For V₃S_n ($n \geq 5$), the cluster can ionize before the fragmentation of neutral species occurs; however, as discussed for V₂S₄⁺ and V₂S₅⁺, the ionic species V₃S_n⁺ can fragment easily (within 20 ns for V₃S₇⁺) and will not be detected by the mass spectrometer. One can conclude that the inability to observe sulfur rich clusters (Fig. 1) through 193 nm laser ionization is due to the low dissociation energy of V_mS_n^{0/+} and insufficient 193 nm photon energy to yield a single photon ionization.

The observation of some sulfur rich clusters (middle panel of Fig. 5) such as VS₃ and VS₄ by cluster ionization through 226 nm (5.49 eV) femtosecond (~ 200 fs) laser radiation supports the above interpretation of cluster fragmentation. For very short laser pulses with high photon fluence, neutral cluster dissociation (Table V) and probably IVR are

TABLE IV. Dissociation channels (only two channels with the lowest dissociation energies are listed for each cluster) and energies (ΔE in eV) of cationic vanadium sulfide clusters.

| | Channel | ΔE | | Channel | ΔE | | Channel | ΔE |
|------------------------------|----------------------------|------------|--|------------------------------|------------|--|-------------------------------|------------|
| VS ⁺ | $\rightarrow V^+ + S$ | 4.47 | V ₂ S ⁺ | $\rightarrow V^+ + VS$ | 4.21 | V ₃ S ⁺ | $\rightarrow V_2^+ + VS$ | 3.81 |
| | $\rightarrow S^+ + V$ | 7.47 | | $\rightarrow VS^+ + V$ | 4.71 | | $\rightarrow V_2S^+ + V$ | 3.93 |
| VS ₂ ⁺ | $\rightarrow V^+ + S_2$ | 3.95 | V ₂ S ₂ ⁺ | $\rightarrow VS^+ + VS$ | 4.71 | V ₃ S ₂ ⁺ | $\rightarrow V_2S_2^+ + V$ | 4.74 |
| | $\rightarrow VS^+ + S$ | 4.00 | | $\rightarrow V^+ + VS_2$ | 4.72 | | $\rightarrow V_2S^+ + VS$ | 4.74 |
| VS ₃ ⁺ | $\rightarrow VS^+ + S_2$ | 2.49 | V ₂ S ₃ ⁺ | $\rightarrow V_2S_2^+ + S$ | 4.58 | V ₃ S ₃ ⁺ | $\rightarrow V_3S_2^+ + S$ | 4.81 |
| | $\rightarrow VS_2^+ + S$ | 3.01 | | $\rightarrow VS^+ + VS_2$ | 4.84 | | $\rightarrow V_2S_3^+ + V$ | 4.97 |
| VS ₄ ⁺ | $\rightarrow VS_2^+ + S_2$ | 2.27 | V ₂ S ₄ ⁺ | $\rightarrow V_2S_3^+ + S$ | 3.51 | V ₃ S ₄ ⁺ | $\rightarrow V_3S_3^+ + S$ | 5.87 |
| | $\rightarrow S_2^+ + VS_2$ | 3.45 | | $\rightarrow V_2S_2^+ + S_2$ | 3.57 | | $\rightarrow V_2S_2^+ + VS_2$ | 6.00 |
| VS ₅ ⁺ | $\rightarrow VS_3^+ + S_2$ | 3.45 | V ₂ S ₅ ⁺ | $\rightarrow V_2S_3^+ + S_2$ | 2.33 | V ₃ S ₅ ⁺ | $\rightarrow V_3S_4^+ + S$ | 3.31 |
| | $\rightarrow VS_2^+ + S_3$ | 4.07 | | $\rightarrow V_2S_4^+ + S$ | 3.34 | | $\rightarrow V_3S_3^+ + S_2$ | 4.65 |
| VS ₆ ⁺ | $\rightarrow VS_4^+ + S_2$ | 2.89 | V ₂ S ₆ ⁺ | $\rightarrow V_2S_4^+ + S_2$ | 1.46 | V ₃ S ₆ ⁺ | $\rightarrow V_3S_4^+ + S_2$ | 2.55 |
| | $\rightarrow VS_5^+ + S$ | 3.22 | | $\rightarrow V_2S_3^+ + S_3$ | 2.59 | | $\rightarrow V_3S_5^+ + S$ | 3.76 |
| | | | | | | V ₃ S ₇ ⁺ | $\rightarrow V_3S_5^+ + S_2$ | 2.99 |
| | | | | | | | $\rightarrow V_3S_6^+ + S$ | 3.75 |

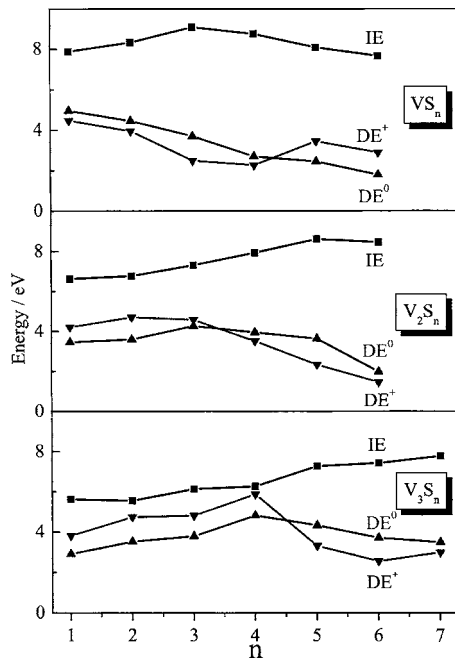


FIG. 10. Ionization energy (IE, solid square), neutral cluster dissociation energy (DE^0 , solid up triangle), and cationic cluster dissociation energy (DE^+ , solid down triangle) of VS_n (top panel), V_2S_n (middle panel), and V_3S_n (bottom panel) are presented. See text for details.

not fast enough to compete with the second (third, etc.) photon absorption and ionization. As a result, more clusters are observed. Nevertheless, clusters can absorb enough excess energy during or after the ionization and fragment due to low dissociation energies of the ion (Table IV). Thus the full (true) cluster distribution is only observed in these experiments by a low fluence, SPI employing a 118 nm (10.5 eV) laser ionization source (bottom panel of Fig. 5).

Sulfur rich clusters have IEs in the range of 7.3–9.1 eV (Table II) which are all below the 118 nm laser single photon energy (10.5 eV). Only 1–3 eV excess energy may be left in the ion. In addition, the photoelectron generated from SPI is likely to take away most of the excess energy, as demonstrated by the study of ionization of V_mO_n , Nb_mO_n , and Ta_mO_n clusters through a 26.5 eV (46.9 nm) soft x-ray laser.¹⁰ As a result, the V_mS_n^+ generated through 10.5 eV SPI can be detected as stable species without fragmentation. The cationic cluster distribution presented in Fig. 2 should represent a real *neutral* cluster distribution, with the possible modulation of relative mass channel intensities, due to the ionization efficiency at 118 nm. Note, however, that one typically observes 118 and 46.9 nm ionizations to yield very similar parent ion distribution patterns.¹⁰

Another interesting point revealed by VUV laser ioniza-

tion is that many hydrogen containing clusters ($\text{V}_m\text{S}_n\text{H}_x$, $x \neq 0$, see Figs. 2 and 3) are formed by the reaction of seeded H_2S with the laser ablation generated vanadium plasma. None of these clusters are observable by ionization through the 193 nm UV laser (see Fig. 1) due to fragmentation. If the results generated by the VUV laser were not available, the UV laser results could be interpreted as a complete dehydrogenation reaction between H_2S and the vanadium plasma. Nitride cluster formation, through the reaction of NH_3 with $\text{Ti}/\text{Zr}/\text{Nb}$ plasmas, has been studied⁴² and one finds that many hydrogen containing cationic clusters such as $\text{TiNH}(\text{NH}_3)_6^+$, $\text{ZrN}(\text{NH}_3)_6^+$, and $\text{NbN}(\text{NH}_3)_4^+$ are formed and detected directly without additional ionization by a mass spectrometer. On the other hand, 355 nm laser postionization was used to detect neutral clusters with no observation of any hydrogen containing species. Aided by laser fluence studies⁴³ and experimental condition arguments, complete dehydrogenation is suggested for the reaction of ammonia with metal plasmas for neutral cluster formation. The results in the present work suggest an alternative interpretation: The inability to observe hydrogen containing neutral clusters by 335 nm postionization⁴² may be due to neutral parent cluster fragmentation through the absorption of a number of 355 nm UV laser photons.

B. V_mS_n cluster stability

As shown in Fig. 2, the most abundant neutral clusters generated are sulfur rich clusters (V_mS_n , $n > m+1$). These clusters are detected, however, as sulfur poor cationic species (V_mS_n^+ , $n \leq m+1$, see Fig. 1) by MPI through 193 nm radiation. Based on the discussion of the cluster fragmentation during ionization in the previous subsection, the mass spectral distribution of cluster ions in Fig. 1 can be assumed to reflect the stability of cationic species: V_nS_n^+ and some $\text{V}_n\text{S}_{n+1}^+$ ($n=3, 5$, and 7) are relatively stable vanadium sulfide cations. This is also supported by the 248 nm photodissociation study reported in Ref. 19: (1) V_mS_n^+ cluster ($n > m+1$) loses S_2 or several S_2 units until $n=m$ or $n=m+1$ upon UV photon absorption; and (2) V_2S_2^+ , V_3S_4^+ , and V_4S_4^+ are found to be very stable. All the experimental results for the cationic species are supported by or support the calculations in this work (see Table IV): (1) the lowest dissociation energies of V_2S_2^+ (4.71 eV), V_3S_4^+ (4.81 eV), and V_4S_4^+ (5.87 eV) are relatively high; and (2) the V_mS_n^+ ($n > m+1$) dissociation channels involving the loss of S_2 have low dissociation energy (<3.6 eV). The calculated dissociation energy of V_3S_4^+ is higher than the 248 nm photon energy (5.00 eV). This should explain the high stability of V_3S_4^+ found in the 248 nm photodissociation study. The lowest energy structure

TABLE V. Dissociation rate constants (s^{-1}) of $\text{V}_m\text{S}_n^{0/+}$ after the cluster absorbs one 193 nm photon. The lowest ΔE value of each cluster in Tables III and IV is used in calculating the dissociation rate.

| n | $\text{VS}_n (\times 10^{10})$ | VS_n^+ | n | V_2S_n | V_2S_n^+ | n | $\text{V}_3\text{S}_n (\times 10^6)$ | V_3S_n^+ |
|---|--------------------------------|----------------------|---|------------------------|--------------------------|---|--------------------------------------|--------------------------|
| 3 | 5.8 | 3.0×10^{11} | 4 | 4.3×10^8 | 1.8×10^9 | 5 | 1.3 | 1.5×10^8 |
| 4 | 5.9 | 1.3×10^{11} | 5 | 2.1×10^8 | 1.4×10^{10} | 6 | 5.7 | 9.5×10^8 |
| 5 | 3.0 | 2.1×10^9 | 6 | 1.6×10^{10} | 7.6×10^{10} | 7 | 4.2 | 5.0×10^7 |
| 6 | 5.9 | 2.7×10^9 | | | | | | |

of V_3S_4^+ calculated in this work has a C_{3v} symmetry which also agrees with the DFT calculations in Ref. 25. The good agreement between experimental and calculated results for V_mS_n^+ in general suggests that VS, V_2S_3 , and V_3S_4 (or generally V_nS_{n+1} , $n \geq 2$) are the most stable neutral species (see Table III). The stable bulk (crystal) forms for vanadium sulfides have stoichiometries of V:S=1:1, 2:3, 3:4, 5:8, and 7:8.⁴⁴ This supports the validity of the DFT calculations, although the gas phase and the condensed phase vanadium sulfides may have different bonding properties and structures.

C. Comparison of vanadium sulfide clusters with vanadium oxide clusters

Many differences can be found between V_mS_n and V_mO_n clusters, mainly due to (1) the stronger bonding between V and O [VO bond strength: 6.51 eV (Ref. 45)] than between V and S [VS bond strength: 4.95 eV (Ref. 34)] and (2) longer bond lengths for V and S [VS bond length: 2.0501 Å (Ref. 21)] than for V and O [VO bond length: 1.5893 Å (Ref. 46)]. $\text{V}_m\text{O}_n^{0/+}$ clusters with stoichiometric ratios $n/m = 2.0-2.5$ are most stable, as found in theoretical and experimental studies.^{47,48} As a result of weaker V-S bonding than V-O bonding, $\text{V}_m\text{S}_n^{0/+}$ clusters with lower n values ($n/m = 1.0-1.5$) are most stable: this conclusion is supported by the calculations and experiments presented in this report. For the same reason, V-V metal bonding is much more significant in sulfides than in the corresponding oxides. One indication of this trend is that the V-V bond length is much shorter in V_2S_2 (1.95 Å, Fig. 7 in this work) than in V_2O_2 (2.58 Å, Fig. 1 in Ref. 47). Metal-metal bonding is also evident in condensed phase vanadium sulfides,⁴⁹ which again confirms the DFT calculated structure qualitatively.

The calculated $\text{V}_n\text{-S}$ bond strengths [$E(\text{V}_n) + E(\text{S}) - E(\text{V}_n\text{S})$] are 4.96, 5.40, and 6.17 eV for $n=1$, 2, and 3, respectively. This suggests that sulfur atoms tend to form bonds with more than one vanadium atom. In other words, to form $(3\text{V})\equiv\text{S}$ and $\text{V}-\text{S}-\text{V}$ bonds is more favorable than to form terminal $\text{V}=\text{S}$ bond. This is understandable since the V-S distance is relatively long, and as a result, sulfur can form bonds with multiple vanadium atoms. In contrast, a test calculation using the BPW91/TZVP method indicates that VO has the largest bond strength among $\text{V}_n\text{-O}$ ($n=1$, 2, and 3). Due to the above bonding difference between vanadium sulfides and oxides, the lowest energy structure (model) of each V_mS_n ($m \geq 2$) cluster is usually different from that of V_mO_n as calculated in Ref. 47: for example, (1) the structure of V_2O_n ($n=3-6$) can be described by a four-membered ring-VOVO plus additional V-O terminal bond(s), while the structures of V_2S_3 and V_2S_5 are described as three V-S-V bonds plus additional terminal bonds (Fig. 7), and (2) V_3O_6 (possibly V_3O_4 and V_3O_5) is described by a six-membered ring-VOVOVO plus additional VO terminal bonds, while the structure of V_3S_n ($n=4$) is characterized by one $(3\text{V})\equiv\text{S}$ bond plus additional V-S-V and V=S bonds (Fig. 8), in agreement with the relatively high V₃-S bond strength.

VI. CONCLUSION

The ionization energies of V_mS_n ($n > m+1$) are around 7–9 eV. The multiphoton ionization of these clusters through 193 nm (6.42 eV) radiation causes severe cluster fragmentation. Although fragmentation depends on many factors, such as absorption and ionization cross sections for particular clusters and laser wavelengths, one may generally conclude that a cluster with a relatively high IE and a low dissociation energy for neutral and/or cationic states is subject to fragmentation in UV multiphoton ionization processes. A real distribution of neutral V_mS_n is detected by single photon ionization through 118 nm (10.5 eV) VUV laser radiation. This technique can be further used to study the reactivity of these neutral clusters. Density functional theory calculations for V_mS_n support and are supported by the experimental observations. The properties and lowest energy structures of V_mS_n and V_mO_n are usually different: (1) V_mO_n are relatively stable with $n/m=2.0-2.5$ while V_mS_n are stable with $n/m=1.0-1.5$; (2) more V-V metallic bonding occurs in sulfide clusters than in the corresponding oxide clusters; and (3) V_mX_n usually has fewer terminal $\text{V}=\text{X}$ bonds and more $\text{V}-\text{X}-\text{V}$ and/or $(3\text{V})\equiv\text{X}$ bonding for $\text{X}=\text{S}$ than for $\text{X}=\text{O}$.

ACKNOWLEDGMENTS

This work was supported by Philip Morris, U.S.A., the U.S. DOE BES program, and the NSF ERC for Extreme Ultraviolet Science and Technology under NSF Award No. 0310717.

- ¹N. Balabanov and K. A. Peteson, J. Chem. Phys. **123**, 064107 (2005).
- ²Y. Zhao and D. G. Truhlar, J. Chem. Phys. **124**, 224105 (2006).
- ³P. B. Armentrout, Annu. Rev. Phys. Chem. **52**, 79 (2001).
- ⁴R. A. J. O'Hair and G. N. Khairallah, J. Cluster Sci. **15**, 331 (2004).
- ⁵Y. Matsuda and E. R. Bernstein, J. Phys. Chem. A **109**, 314 (2005).
- ⁶Y. Matsuda, D. N. Shin, and E. R. Bernstein, J. Chem. Phys. **120**, 4142 (2004).
- ⁷Y. Matsuda and E. R. Bernstein, J. Phys. Chem. A **109**, 3803 (2005).
- ⁸D. N. Shin, Y. Matsuda, and E. R. Bernstein, J. Chem. Phys. **120**, 4157 (2004).
- ⁹Y. Matsuda, D. N. Shin, and E. R. Bernstein, J. Chem. Phys. **120**, 4165 (2004).
- ¹⁰F. Dong, S. Heinbuch, S.-G. He, Y. Xie, J. J. Rocca, and E. R. Bernstein, J. Chem. Phys. **125**, 164318 (2006).
- ¹¹S.-G. He, Y. Xie, F. Dong, S. Heinbuch, E. Jakubikova, J. J. Rocca, and E. R. Bernstein (unpublished).
- ¹²M. Lacroix, N. Boutarfa, C. Guillard, M. Vrinat, and M. Breysse, J. Catal. **120**, 473 (1989).
- ¹³C. Guillard, M. Lacroix, M. Vrinat, M. Breysse, B. Mocaire, J. Grimbrot, T. des Courieres, and D. Faure, Catal. Today **7**, 587 (1990).
- ¹⁴T. J. Carlin, M. B. Wise, and B. S. Freiser, Inorg. Chem. **20**, 2743 (1981).
- ¹⁵I. Dance, K. Fisher, and G. Willett, Angew. Chem., Int. Ed. Engl. **34**, 201 (1995).
- ¹⁶I. G. Dance, K. J. Fisher, and G. D. Willett, Inorg. Chem. **35**, 4177 (1996).
- ¹⁷I. Kretzschmar, D. Schroder, and H. Schwarz, C. Rue, and P. B. Armentrout, J. Phys. Chem. A **102**, 10060 (1998).
- ¹⁸I. Kretzschmar, D. Schroder, H. Schwarz, and P. B. Armentrout, Int. J. Mass. Spectrom. **228**, 439 (2003).
- ¹⁹W.-J. Wang, P. Liu, D.-B. Hu, Z. Gao, F.-A. Kong, and Q.-H. Zhu, Chin. J. Chem. Phys. **10**, 110 (1997).
- ²⁰K. Fisher, I. Dance, G. Willett, and M. N. Yi, J. Chem. Soc. Dalton Trans. **1996**, 709.
- ²¹Q. Ran, W. S. Tam, A. S.-C. Cheung, and A. J. Merer, J. Mol. Spectrosc. **220**, 87 (2003).

- ²² B.-Y. Liang and L. Andrews, J. Phys. Chem. A **106**, 3738 (2002).
- ²³ Y. Steudel, M. W. Wong, and R. Steudel, Eur. J. Inorg. Chem. **2005**, 2514.
- ²⁴ X.-G. Xie, S.-L. Gao, and J.-L. Xu, J. Mol. Struct.: THEOCHEM **715**, 65 (2005).
- ²⁵ S.-F. Wang, J.-K. Feng, M. Cui, M.-F. Ge, C.-C. Sun, Z. Gao, and F.-A. Kong, Gaodeng Xuejiao Huaxue Xuebao (Chem. J. Chinese Univ.; ISSN: 0251-0790), **20**, 1447 (1999).
- ²⁶ D. N. Shin, Y. Matsuda, and E. R. Bernstein, J. Chem. Phys. **120**, 4150 (2004).
- ²⁷ S.-G. He, Y. Xie, F. Dong, and E. R. Bernstein, J. Chem. Phys. **125**, 164306 (2006).
- ²⁸ A. D. Becke, Phys. Rev. A **38**, 3098 (1988).
- ²⁹ J. P. Perdew and Y. Wang, Phys. Rev. B **45**, 13244 (1991).
- ³⁰ A. Schaefer, C. Huber, and R. Ahlrichs, J. Chem. Phys. **100**, 5829 (1994).
- ³¹ M. J. Frisch, G. W. Trucks, H. B. Schlegel *et al.*, GAUSSIAN 03, Revision C.02 (Gaussian, Inc., Wallingford, CT, 2004).
- ³² E. M. Spain, J. M. Behm, and M. D. Morse, J. Chem. Phys. **96**, 2511 (1992).
- ³³ A. M. James, P. Kowalczyk, E. Langlois, M. D. Campbell, A. Ogawa, and B. Simard, J. Chem. Phys. **101**, 4485 (1994).
- ³⁴ J. P. Botor and J. G. Edwards, J. Chem. Phys. **81**, 2185 (1984).
- ³⁵ K. A. Peterson, J. R. Lyons, and J. S. Francisco, J. Chem. Phys. **125**, 084314 (2006).
- ³⁶ C. Liao and C. Ng, J. Chem. Phys. **84**, 788 (1986).
- ³⁷ E. Picquenard, O. El Jaroudi, and J. Corset, J. Raman Spectrosc. **24**, 11 (1993).
- ³⁸ P. Hassanzadeh and L. Andrews, J. Phys. Chem. **96**, 6579 (1992).
- ³⁹ J. Berkowitz and C. Lifshitz, J. Chem. Phys. **48**, 4346 (1968).
- ⁴⁰ A. K. Wilson and T. H. Dunning, Jr., J. Chem. Phys. **119**, 11712 (2003).
- ⁴¹ E. Jakubikova, A. K. Rappe, and E. R. Bernstein, J. Phys. Chem. A **110**, 9529 (2006).
- ⁴² S. E. Kooi and A. W. Castleman, Jr., Chem. Phys. Lett. **315**, 49 (1999).
- ⁴³ B. C. Guo, S. Wei, Z. Chen, K. P. Kerns, J. Purnell, S. Buzzia, and A. W. Castleman, Jr., J. Chem. Phys. **97**, 5243 (1992).
- ⁴⁴ W. Bensch and R. Schlogl, J. Solid State Chem. **107**, 43 (1993).
- ⁴⁵ G. Baldacci, G. Gigli, and M. Guido, J. Chem. Phys. **79**, 2351 (1983).
- ⁴⁶ K. P. Huber and G. Herzberg, *Molecular Spectra and Molecular Structure. IV. Constants of Diatomic Molecules* (Van Nostrand Reinhold, New York, 1979).
- ⁴⁷ M. Calatayud, J. Andres, and A. Beltran, J. Phys. Chem. A **105**, 9760 (2001).
- ⁴⁸ K. S. Molek, T. D. Jaeger, and M. A. Duncan, J. Chem. Phys. **123**, 144313 (2005).
- ⁴⁹ W. B. England, S. H. Liu, and H. W. Myron, J. Chem. Phys. **60**, 3760 (1974).